

FUSED ULTRA WIDEBAND RADIO, COMMUNICATIONS, AND RADAR WITH MEMS AIDING FOR INDOOR NAVIGATION AND COLLISION AVOIDANCE

Brandon S. Dewberry*

Pulsed Ultra Wideband (UWB) ranging and communications is a proven technology for indoor and GPS-compromised localization and peer-to-peer proximity safety systems. Recent results provide a strong basis for its capability as short-range radar for proximity detection. In this research the relative pose of a small UWB radar estimated by a combination of UWB TW-TOF ranging combined with inertial sensing. Sequential UWB radar scans are combined using back-propagation synthesis to form a sequence of Synthetic Aperture Radar (SAR) images. The resulting dynamic images reveal collision hazards and mapping targets suitable for both safe guidance and SLAM processing.

INTRODUCTION

Recent interest in unmanned vehicles has motivated development of novel sensors for navigation and collision avoidance that are able to operate in complex environments. While the utility of Ultra Wideband RF techniques for indoor localization is well-established^{1,2}, as well as UWB radar for person tracking^{3,4}, the fusion of both modes in one small sensor could produce a sensor ideal for use in small vehicle autonomy.

Radars are now common on ground vehicles for automatic cruise control and collision warning. These radars detect the distance and relative speed of targets in the antenna field of view^{5,6}. Newer short-range UWB radar sensors have been recently added as parking aids, back-up warning, lane changing, and emergency braking. These radars likewise detect distance to first target in their field of view with more advanced systems combining multiple overlapping fields into images⁷. These techniques differ from Synthetic Aperture Radar (SAR), which requires motion tangentially across the measurement scene, and combining continuously collected range profiles into a cohesive image.

Pulsed-RF UWB radar has been shown to work well detecting and tracking people indoors in high clutter environments⁸. Detections generated by an array of such sensors can be combined to track people in an office environment⁹. This indicates that multiple scans from the sensor could be combined for imaging and collision avoidance, even in high clutter.

* Time Domain, 4955 Corporate Dr., Huntsville, AL 35805.

SAR imaging techniques are typically used on large manned and unmanned aircraft^{10,11}. In fact the signal type and phenomenology is strikingly similar to underwater sonar, which provides a direct-sampled reflectivity scan at resolution greater than Nyquist. Thus the techniques applied are informed directly from underwater sonar imaging¹² which uses straightforward back-projection mapping across sensor motion.

UWB radar sensors have decreased in size, weight, and power consumption initiating a growing number of investigations promoting its use on small, unmanned drones for augmenting optical imagery in scientific, agricultural, and environmental monitoring^{13,14}. These techniques depend on a straight-line trajectory across the measurement scene with side-view or bottom-mounted look-angles. Others are simply deriving a robust measure of altimetry¹⁵. This investigation suggests these techniques can be expanded for higher precision and ease given active recursive pose estimation through UWB Two Way Ranging on the same sensor, and with targeted platform behaviors specifically at improving image resolution and feature extraction.

In order to provide coherent image formation back-projection SAR algorithm requires high navigational accuracy proportional to the radar frequency band. It also requires a high radar scan rate related to vehicle speed for reduction of side-lobe effects. This report provides an assessment of these trade-offs using both simulated and experimental evidence.

MEASUREMENT SYSTEM

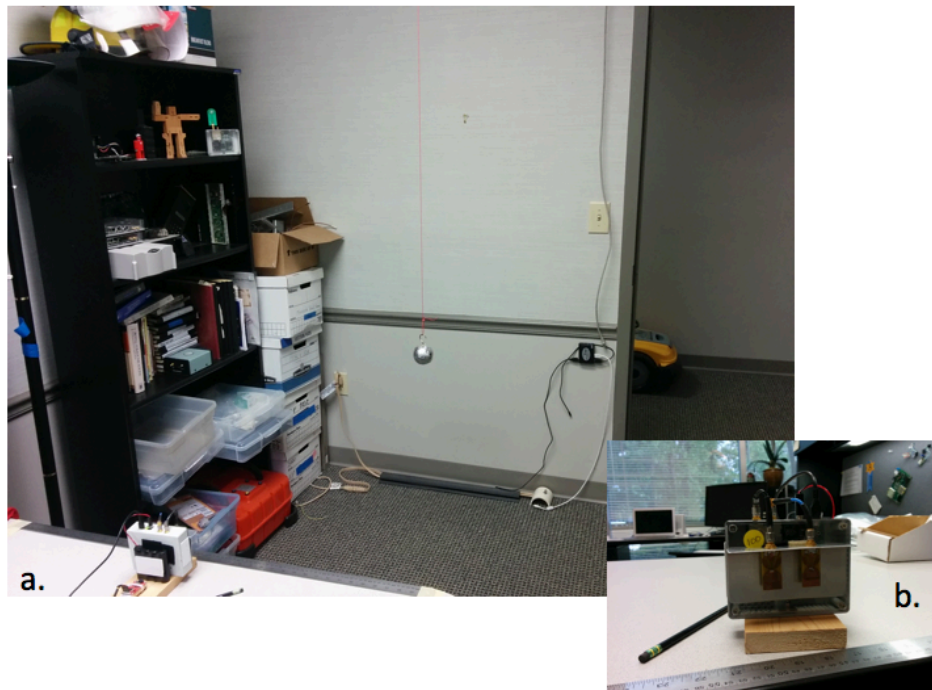


**Figure 1 a. View of test volume from above and behind the radar's perspective.
b. The front of the radar showing dual back-reflected antennas.**

Figure 1a provides a broad view of the test volume (a cluttered 3m wide office.) The radio-radar unit in the bottom left was moved left to right on the desktop while range and radar data

was collected through its USB connection. One of the two reference radios can be seen on the bookshelf at the top left (a robot is pointing to it.) The other reference radio is out of view on the right side wall past the open door. A 7.5 cm diameter foil-covered baseball was used for radar range calibration and resolution assessment.

A front view of the radio-radar is presented in figure 1b. The sensor is a Time Domain P410 module augmented with dual back-reflected UWB antennas. Data was collected through high speed USB connection and post-processed using Matlab.

A dual back-reflected antenna was used on the sensor in order to provide a forward-facing pattern of approximately 120° in the azimuth plane, greatly reducing the effect of reflective clutter from behind the platform. The directional antenna simply consists of an aluminum sheet with bend with holes drilled for SMA bulkhead holding the antenna elements parallel to the reflective plane at a separation distance of $\frac{1}{4}\lambda_c = 18$ mm.

LOCALIZATION

An Extended Kalman Filter (EKF) used for localization of the platform based on distance measurements to a static radios at surveyed locations as reported previously¹. Linearization of the observation matrix, H , is used to solve in Cartesian coordinates while measuring in polar. The mobile platform is tracked in 2D at the in the plane of the mobile platform, taking into account the heights of the anchor nodes.

$$\hat{X}_{k|k-1} = F_k(\delta t)\hat{X}_{k-1|k-1} \quad (1)$$

$$C_{k|k-1} = F_k(\delta t)C_{k-1|k-1}F_k^T(\delta t) + Q(\sigma_{accel}^2) \quad (2)$$

$$\tilde{r}_k = \sqrt{(\hat{x}_{k|k-1} - x^a)^2 + (\hat{y}_{k|k-1} - y^a)^2 + (z_m - z^a)^2} \quad (3)$$

$$H_k = \left[\frac{\hat{x}_{k|k-1} - x^a}{\tilde{r}_k}, 0, \frac{\hat{y}_{k|k-1} - y^a}{\tilde{r}_k}, 0 \right] \quad (4)$$

$$K_k = C_{k|k-1}H_k^T / (HC_{k|k-1}H_k^T + \sigma_{r_m}^2) \quad (5)$$

$$\hat{X}_{k|k} = \hat{X}_{k|k-1} + K_k(r_m - \tilde{r}_k) \quad (6)$$

$$C_{k|k} = (I - K_kH_k)C_{k|k-1} \quad (7)$$

Where δt is the time since last update, σ_{accel}^2 is the tuned acceleration variance, (x^a, y^a, z^a) is the location of the anchor radio associated with the range measurement r_m , and z_m is the (assumed constant) height of the mobile platform. Thus the anchor locations (x^a, y^a) define the orientation of the navigation plane, while the platform height z_m defines the height of the navigation and imaging plane.

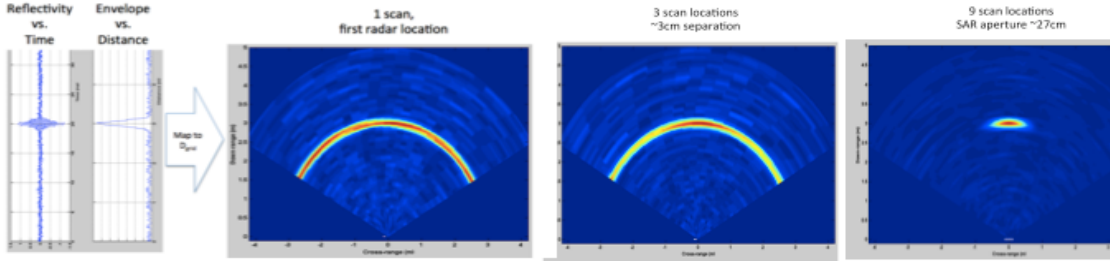


Figure 2. Iterative mapping of UWB scan to distance to 2D plane across a 9 step track from -.

IMAGING

As depicted in figure 2, images are derived through combination of a window of scans using a back projection technique commonly used by larger radar and underwater sonar⁸. The technique is similar to The UWB sensor provides equivalent-time sampled vectors representing the reflectivity amplitudes versus discrete time $s(t_k)$ with $t_{k+1}-t_k = 61\text{ps}$. As a first step the amplitudes are mapped to range bins using the identity $s(r_k) = s(c \cdot t_k / 2)$, where c is the speed of light. In addition the signal envelope or Energy-Time Curve (ETC) is found using the absolute value of its Hilbert transform¹².

The reflectivity vector $s(r_k)$ is mapped to Cartesian coordinates by first constructing a matrix $D_{i,j}$ containing the distances from the sensor location of that element from the dynamic sensor location

$$D_{i,j,k} = \sqrt{(x_{i,j} - x_k)^2 + (y_{i,j} - y_k)^2 + (z_{i,j} - z_k)^2}$$

where (x_k, y_k, z_k) is the location of the sensor at time k and $x_{i,j}$, $y_{i,j}$, and $z_{i,j}$ are pre-computed matrices reflecting the dimensional grid point distance to a common horizontal frame origin.

A image from a single radar scan at time k is formed through the $\mathbb{R}^1 \rightarrow \mathbb{R}^2$ mapping $\text{IMG} = s_k(D_{i,j,k})$ and the synthetic aperture image formed through windowed average summation

$$\text{IMG}_k = \frac{1}{n} \sum (s_{k-n}, s_{k-n+1}, \dots, s_k)$$

The trailing window of size k can be dynamically adjusted based on velocity and aperture (cross-range resolution) requirements.

RESULTS

Figure 4 depicts an image gathered in a typical office environment. During a ~ 10 second operational window with the sensor moved across 0.6 meters in the positive x direction with minimal variation in y , and constant z height (slid across a desk.)

Scans were gathered at an average of 2 Hz and 3 cm. Between each scan the sensor ranged to one of the two static anchor reference nodes at surveyed coordinates relative to the imaging and navigation frame. The 7.5 cm diameter calibration sphere can be seen clearly in the image, along with other targets and features as annotated in the image.

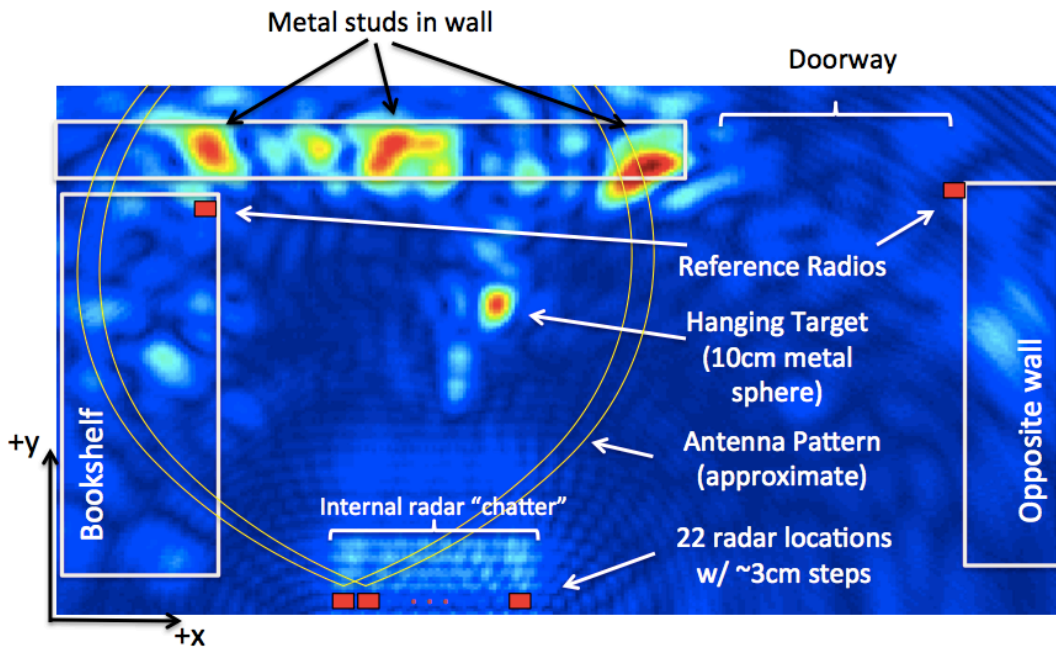


Figure 4. A typical navigation and SAR imaging result in a cluttered volume. Pertinent features are annotated in the image.

DISCUSSION

As indicated in figure 4 the frequency band of the radar (3.1 to 5.1GHz) presents high return strength on metal objects, such as the aluminum studs inside the office wall structure. These highly reflective targets can overpower structures, which pass microwave energy - such as the gypsum board covering the studs. There are several options for reducing this effect, which simply indicates a wide dynamic range. However this may also reveal an advantage when defining features for SLAM navigation.

A mix of both localization and radar error dictates image resolution. Localization error is a combination of UWB Two-Way Ranging (TWR) error and Geometric Dilution of Precision (GDOP). The TWR error was found to be approximately 2 cm, an expansion of typical LOS ranging error due to antenna back-reflector effects.

There is a trade-off between antenna requirements for ranging and navigation. Typically omnidirectional radio antennas are used in support of localization and communications. However directional antennas are typically required for radar in order to reduce clutter from behind the platform. Fused localization and sensing requires less electronics but introduces anchor availability and GDOP issues. To counter this effect one may either 1) use multiple directional antennas connected through a RF switch (reducing the scan rate) or 2) multiple radio-radars directed outward in overlapping quadrants around the vehicle, with parallel scanning/ranging, or 3) separating the radar and ranging functions into multiple devices. Future experiments will compare these methods.

Back-reflecting an omnidirectional UWB antenna changes the phase center / group delay of the received signal. This modifies the bias of the TWR solution by a small amount causing error

in the navigation solution when using anchors at obtuse angles. Although small, this error could be reduced by adjusting range bias based on orientation from sensor to anchor.

The group delay changes caused by back-reflection also manifests as a decrease in radar resolution of reflections at obtuse angles. Thus SAR process will cause a decrease in radar cross-range resolution, and targets towards the outer edges of the antenna pattern will be “fuzzy” compared to frontwards targets. Introducing platform control behaviors that rotate the sensor to point towards the closest target (“staring” at the target while moving around it) would reduce this effect.

SAR techniques increase the effective aperture (and cross-range resolution) through controlled movement in a dimension orthogonal to target. Forward-mounted radar can detect an obstacle but active sideways motion is required for isolation of its size. Single radar with high directionality may be most suitable for platforms with strafing capability such as multicopters or those with mecanum wheels. In high clutter environments a small array may be required to provide some bearing information for downrange targets. The array size can be kept small (two or three radar front ends) if supported by vehicle inspection behavior.

The user configures maximum radar distance. In practice the radar range equation will limit the maximum practical range based on target return and update rate required relative to the speed of the platform. In addition in this sensor the measurement latency increases with configured max distance due to equivalent time sampling and coherent integration. For adequate interferometric beamforming on a moving vehicle the scan rate should support measurement separations close to $\frac{1}{4} \lambda_c \sim 3\text{cm}$ in order to reduce side lobe effects. Thus, in this study $r_{\text{max}} = \sim 5\text{ m}$ was chosen in an effort to target close-proximity collision avoidance in indoor environments at relatively fast movement rates. In open spaces r_{max} could be dynamically reconfigured and non-coherent non-interferometric operations used at the expense of cross-range resolution.

Reflections of RF combined with limited dynamic range of the sampler caused noise artifacts in the first meter or so from the sensor. This is reduced but not eliminated through SAR processing, but may cause an increase in the probability of false detection of close targets. RF front end and antenna adjustments could reduce this effect as well as a parallel motion filtering process may reduce the false detection of close-in targets.

The range and resolution of using this technique should be adequate to support feature extraction for Simultaneous Localization and Mapping (SLAM.) SLAM techniques are quite similar to localization based on active Two-Way Ranging and it should be straightforward to mix SLAM with active UWB EKF localization allowing a sparse deployment of UWB anchor nodes. This will be explored in a future investigation.

CONCLUSION

Fused UWB ranging and radar can enable both navigation and mapping in high multipath environments using a single, small sensor package. The pulsed basis provides for both precision recursive localization in high multipath as well as radar sensing in close proximity and high clutter rejection. However while an omnidirectional antenna pattern is ideal for navigation and communication, a directional pattern is best for radar sensing. Multiple sensors around the platform with intelligent selection and processing may be required to solve this discrepancy. This would also allow parallel scanning for faster update rate and instantaneous bearing information in the down-range direction – the subject of future investigations.

REFERENCES

- ¹ B. Dewberry and M. Einhorn, "Ad-hoc autosurvey with precision local navigation of mobile platforms using a peer-to-peer ranging network," *Unmanned Systems 2014 Proceedings of the AUVSI Conference on*, 12-15 May, 2014.
- ² B. Silva et al. "Experimental study of UWB-based high precision localization for industrial applications," *Ultra-WideBand (ICUWB), 2014 IEEE International Conference on*, vol., no., pp.280,285, 1-3 Sept. 2014
- ³ S. Chang, R. Sharan, M.Wolf, N. Mitsumoto, and J.W. Burdick, "People Tracking with UWB Radar Using a Multiple-Hypothesis Tracking of Clusters (MHTC) Method," in *Int J Soc Robot* (2010) 2. Springer, Jan. 2010, p. 318.
- ⁴ Kocur, D.; Novak, D.; Rovnakova, J., "Moving person tracking by UWB radar system in complex environment," *Intelligent Signal Processing (WISP), 2013 IEEE 8th International Symposium on*, vol., no., pp.77,82, 16-18 Sept. 2013.
- ⁵ H. Rohling "Milestones in radar and the success story of automotive radar systems", *Proc. 11th Int. Radar Symp.*, pp.1 -6 2010.
- ⁶ Rollmann, G., Schmid, V. Mekhaie, M. And P. Knoll, "Short Range Radar System for Automotive Applications, "Advanced Microsystems for Automotive Applications, 215-221, 2003.
- ⁷ Wenger, J.; Hahn, S., "Long Range and Ultra-Wideband Short Range Automotive Radar," *Ultra-Wideband, 2007. ICUWB 2007. IEEE International Conference on*, vol., no., pp.518,522, 24-26 Sept. 2007.
- ⁸ Kilic, Y.; Wymeersch, H.; Meijerink, A.; Bentum, M.J.; Scanlon, W.G., "Device-Free Person Detection and Ranging in UWB Networks," *Selected Topics in Signal Processing, IEEE Journal of*, vol.8, no.1, pp.43,54, Feb. 2014.
- ⁹ B. Gulmezoglu, M. B. Guldogan, and Sinan Gezici, "Multiperson tracking with a network of ultra wideband radar sensors based on Gaussian mixture PHD filters," *IEEE Sensors Journal*, vol 15, no. 4, April 2015.
- ¹⁰ L. M. H. Ulander, H. Hellsten, and G. Stenstrom, "Synthetic-aperture radar processing using fast factorised back-projection," *IEEE Trans. Aerospace and Electronic Systems*, 2001.
- ¹¹ Rosen, P. A., S. Hensley, K. Wheeler, G. Sadowy, T. Miller, S. Shaffer, R. Muellerschoen, C. Jones, S. Madsen, and H. Zebker, "UAVSAR: Airborne SAR system for research," *IEEE A&E Systems Magazine*, 21-28, 2007.
- ¹² Lyons, Anthony, et al. "Seafloor measurements using synthetic aperture sonar." *Proceedings of Meetings on Acoustics*. Vol. 19. No. 1. Acoustical Society of America, 2013.
- ¹³ V. C. Koo, et al, "A new unmanned aerial vehicle synthetic aperture radar for environmental monitoring," *Progress In Electromagnetics Research*, Vol. 122, 245-268, 2012.
- ¹⁴ J. Nikolic, and D. Brescianini. "Ultra Wideband Radar for Micro Aerial Vehicles." Thesis, ETH Zurich Autonomous Systems Lab, Autumn 2009, http://students.asl.ethz.ch/upl_pdf/173-report.pdf.
- ¹⁵ Saldana, R. R. and F. P. Martinez, "Design of a millimetre synthetic aperture radar (SAR) onboard UAV's ," *IEEE International Conference on Electronics, Circuits and Systems*, 1-5, 2007.